

Diffusion Transients in Convection Rolls

Qingqing Yin¹, Yunyun Li¹†, Baowen Li², Fabio Marchesoni^{1,3}, Shubhadip Nayak⁴ and Pulak K. Ghosh⁴‡

¹Center for Phononics and Thermal Energy Science, Shanghai Key Laboratory of Special Artificial Microstructure Materials and Technology, School of Physics Science and Engineering, Tongji University, Shanghai 200092, China

²Paul M. Rady Department of Mechanical Engineering and Department of Physics, University of Colorado, Boulder, Colorado 80309-0427, USA

³Dipartimento di Fisica, Università di Camerino, I-62032 Camerino, Italy

⁴Department of Chemistry, Presidency University, Kolkata 700073, India

(Received xx; revised xx; accepted xx)

We numerically investigated the phenomenon of non-Gaussian normal diffusion of a Brownian colloidal particle in a periodic array of planar counter-rotating convection rolls. At high Péclet numbers, normal diffusion is observed to occur at all times with non-Gaussian transient statistics. This effect vanishes with increasing the observation time. The displacement distributions decay either slower or faster than a Gaussian function, depending on the flow parameters. The sign of their excess kurtosis is related to the difference between two dynamical time scales, namely, the mean exit time of the particle out of a convection roll and its circulation period inside it.

Key words: Brownian motion, Diffusion, Non-Gaussian distribution.

1. Introduction

Fick's diffusion (Gardiner 2009) implies that the directed displacements of an overdamped Brownian particle, say, in the x direction, $\Delta x(t) = x(t) - x(0)$, grow with time following the Einstein law, $\langle \Delta x^2(t) \rangle = 2Dt$, and with Gaussian statistics. Accordingly, the probability density function (pdf) of the rescaled observable, $\Delta x/\sqrt{t}$, would be a stationary Gaussian distribution with half-variance D .

Recent observations (Wang et al. 2009, 2012; Bhattacharya et al. 2013; Kim et al. 2013; Kwon et al. 2014; Guan et al. 2014) of Brownian motion in fluctuating crowded environments led to question the generality of such notion. Indeed, there are no *a priori* reasons why the diffusion of a physical Brownian tracer should be of Fickian type. For instance, in real biophysical systems displacement pdf's often exhibit prominent exponential tails over wide intervals of the observation time, t , well after the condition of normal diffusion has set in. Such a transient effect, termed here non-Gaussian normal diffusion (NGND), is expected to disappear for asymptotically large observation times (possibly inaccessible to real experiments (Wang et al. 2009)), as stipulated by the central limit theorem. In that limit, the Δx distributions turn eventually Gaussian, with half-variance equal to $\langle \Delta x^2(t) \rangle$. Persistent diffusive transients of this type have been detected in diverse experimental setups (Wang et al. 2009, 2012; Bhattacharya et al. 2013; Weeks et al. 2000; Eaves et al. 2009; Leptos et al. 2009), and further confirmed by extensive numerical

† Email address for correspondence: yunyunli@tongji.edu.cn

‡ Email address for correspondence: pulak.chem@presiuniv.ac.in

simulations (Kwon et al. 2014; Guan et al. 2014; Keqel et al. 2000; Chaudhuri et al. 2007; He et al. 2016; Ghosh et al. 2016).

The current interpretation of this phenomenon postulates that diffusion occurs in a fluctuating environment with finite relaxation time, τ (Wang et al. 2009). For observation times comparable with τ , the tracer displacements are likely to obey a non-Gaussian statistics. The rescaled pdf's, $p(\Delta x/\sqrt{t})$, are typically Gaussian for either much shorter or much larger t values, though with different half-variance: the free diffusion constant, D_0 , for $t \rightarrow 0$ (no crowding effect) and the asymptotic diffusion constant, D , defined above, for $t \rightarrow \infty$ (central limit theorem). There is no fundamental reason why non-Gaussian transients should necessarily lead to the emergence of slowly decaying distribution tails (leptokurtic transients), as reported in the current literature; on the contrary, one cannot rule out the possibility that, under certain conditions, their tails decay faster than a Gaussian tail (platykurtic transients). Moreover, the NGND phenomenon can also occur in low dimensional models, though restricted to relatively narrow t domains (Li et al. 2019).

We investigate here, both numerically and analytically, the Brownian diffusion of an overdamped particle suspended in a periodic array of planar convection rolls, subjected to thermal fluctuations of strength D_0 . This is an archetypal model with well-established applications to physical systems of the most diverse length scale (Kirby 2010; Tabeling 2002; Chandrasekhar 1967). At high Péclet numbers, i.e., when the effects of thermal fluctuations are negligible with respect to advection, the particle undergoes normal diffusion with asymptotic diffusion constant, D , which depends on both D_0 and the flow parameters (Rosenbluth 1987). The ensuing NGND is characterized by a single transient time, τ , but, in contrast with other elementary models (Li et al. 2019), τ is controlled by two competing microscopic mechanisms depending on D_0 . At low thermal noise, the transient dynamics of the particle is governed by its isotropic random jumps from roll to roll, a stochastic process quite insensitive to the details of the particle's trajectory inside each individual roll. On the contrary, upon raising the thermal noise (but still at high Péclet numbers), roll jumping grows faster compared with the circulation inside the rolls. The diffusion transient dynamics is then dominated by the advective drag. Accordingly, one defines two distinct time scales, namely, the mean time for the particle to first exit the convection rolls and its average revolution period inside a single roll. The peculiarity of this system is that, upon increasing the noise strength, the NGND transients can change from leptokurtic to platykurtic, depending on which of such two time scales is larger and, thus, plays the role of effective transient time, τ .

The problem we address is also of practical interest in view of its applications to microfluidics (Kirby 2010), chemical engineering and combustion (Moffatt et al. 1992), and the modeling of large-scale geodynamic processes (Tabeling 2002). Indeed, the experimental or numerical determination of the asymptotic mean-square displacement of a tracer in a convective flow can take exceedingly long times to allow it to jump repeatedly from convection roll to convection roll. On the contrary, in a number of physical situations the observer only needs to determine how long a trapped tracer will sojourn inside a single roll before crossing its flow boundary layer into a neighboring one. This quantity is more easily accessible to direct observation and, as shown at the end of this paper, influences the non-Gaussian properties of the tracer's transient displacement distributions. Stated otherwise, from displacement distributions obtained for finite observation times, we cannot extract the asymptotic diffusion constant, D , with a high degree of confidence, if the non-Gaussian transients of the underlying diffusive process is unpredictably long.

The present paper is organized as follows. In Sec. 2 we introduce the Langevin equations that describe Brownian diffusion in a two-dimensional laminar flow patterned as a periodic array of counter-rotating convection rolls. Following Ref. (Rosenbluth 1987), we distinguish between the regime of high Péclet numbers, relevant to this work, where diffusion is governed by advection, and the best known regime of thermal diffusion, dominated by equilibrium fluctuations. In Sec. 3 we investigate the two time scales controlling Brownian diffusion in a periodic array of convection

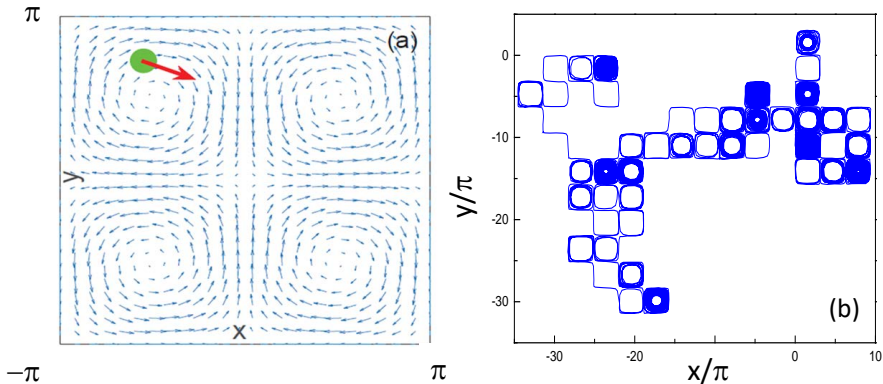


Figure 1: Diffusion of a Brownian particle in a 2D periodic pattern of stationary convection rolls. (a) Unit flow cell, Eq. (2.1), consisting of four counter-rotating subcells. (b) Trajectory sample of length $t=100$, for $D_0 = 0.001$. Flow parameters are: $U_0 = 1$ and $L = 2\pi$.

rolls, namely, the average period of fluid circulation inside a roll (Sec. 3.1) and the particle's mean first-exit time out of a single roll (Sec. 3.2). In Sec. 4 we present detailed numerical evidence of the NGND phenomenon. Lepto- and platykurtic transients are qualitatively explained by time coarse-graining the microscopic particle's dynamics and quantified by fitting our numerical displacement distributions by means of a phenomenological one-parameter function. Finally, in Sec. 5 we draw some concluding remarks.

2. Model: Periodic Array of Counter-rotating Convection Rolls

To this purpose we investigated the diffusion of an overdamped particle of unit mass, coordinates x and y , suspended in a 2D stationary laminar flow with periodic center-symmetric stream function

$$\psi(x, y) = (U_0 L / 2\pi) \sin(2\pi x / L) \sin(2\pi y / L), \quad (2.1)$$

where U_0 is the maximum advection speed and L the size of the flow unit cell. Following the earlier literature (Chandrasekhar 1967; Rosenbluth 1987; Childress 1979; Soward 1987), we assumed that the particle is perfectly spherical and so small that it can be taken as pointlike. Accordingly, away from confining boundaries or other particles (low particle density approximation) hydrodynamic interactions and flow torques were ignored. Its dynamics can thus be formulated by means of two translational Langevin equations,

$$\dot{x} = u_x + \xi_x(t), \quad \dot{y} = u_y + \xi_y(t), \quad (2.2)$$

where the vector $\vec{u} = (u_x, u_y) = (\partial_y, -\partial_x)\psi$ is the advection velocity. As illustrated in Fig. 1(a), $\psi(x, y)$ defines four counter-rotating flow subcells, also termed convection rolls. The translational noises, $\xi_i(t)$ with $i = x, y$ are stationary, independent, delta-correlated Gaussian noises, $\langle \xi_i(t) \xi_j(0) \rangle = 2D_0 \delta_{ij} \delta(t)$. They can be regarded as modeling equilibrium thermal fluctuations in a homogeneous, isotropic medium, with D_0 proportional to its temperature. In the present notation, D_0 is the free particle diffusion constant in the absence of advection. In our simulations, we used the flow parameters, U_0 and L to set convenient length and time units, respectively, L and $L/2\pi U_0$. Therefore, the only tunable parameter left in our analysis is the noise strength, D_0 . As we are interested in the diffusion properties under stationary conditions, we assumed a uniform random distribution of the particle's initial coordinates, x_0 and y_0 . Indeed,

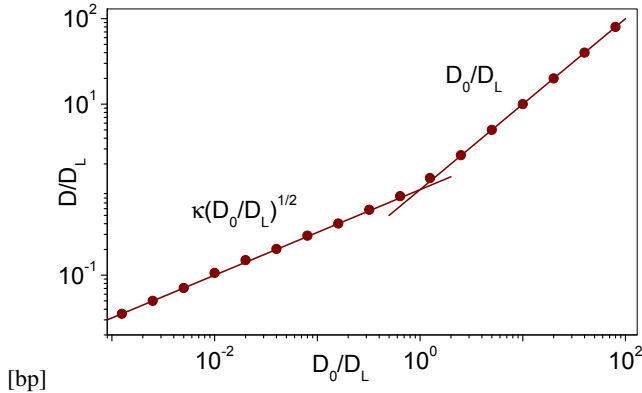


Figure 2: Diffusion in the periodic convective flow pattern of Eq. (2.1): D vs. D_0 , both rescaled by $D_L = U_0 L / 2\pi$. The analytical predictions for low-noise, Eq. (2.4), and high-noise strength, Eq. (2.5), are represented by solid lines. Within our numerical accuracy, the fitted value of κ is consistent with the predicted value, 1.06 (Rosenbluth 1987). The stream function parameters are $U_0 = 1$ and $L = 2\pi$, so that $D_L = 1$.

due to the incompressibility of the advection vector, (u_x, u_y) , in the presence of thermal noise, a particle's trajectory is known to eventually fill up the x, y plane uniformly.

The amplitude of $\psi(x, y)$ in Eq. (2.1) provides a natural diffusion scale of the convective flow, $D_L = U_0 L / 2\pi$; accordingly the Péclet number of the advected Brownian particle is defined here as $\text{Pe} \equiv D_L / D_0 > 1$.

The stochastic differential Eqs. (2.2) were numerically integrated by means of a standard Mil'shtein scheme (Kloeden et al. 1992). Particular caution was exerted when computing the values of the asymptotic diffusion constant

$$D = \lim_{t \rightarrow \infty} \langle \Delta x^2(t) \rangle / 2t. \quad (2.3)$$

Indeed, upon lowering the noise strength, D_0 , the roll jumping of the advected particle gets suppressed; accordingly, the transient time, τ , grows exceedingly long. Even if during such transients instances of anomalous diffusion may become detectable (Young et al. 1989), in this paper we focus on the normal diffusion limit in Eq. (2.3).

Particle transport in such a flow pattern has been studied under diverse physical conditions and a rich phenomenology has emerged (Shraiman 1987; Young et al. 1989; Solomon et al. 1988; Solomon 2003; Young 2007; Manikantan 2013; Sarracino et al. 2016; Tornev et al. 2007; Li et al. 2020). For instance, in the presence of external periodic perturbations the deterministic dynamics of a noiseless particle exhibits remarkable chaotic properties (Solomon et al. 1988; Solomon 2003). Especially relevant to the present work are the results for the diffusivity of a pointlike Brownian tracer first reported in Ref. (Rosenbluth 1987). The problem of how a flow field of stream function $\psi(x, y)$ affects the diffusion of self-propelled particle has been investigated in Refs. (Tornev et al. 2007; Li et al. 2020).

The Langevin Eqs. (2.2) model particle diffusion under the simultaneous action of translational fluctuations and advective drag. An important property of this system is illustrated in Fig. 2, where we plotted the asymptotic diffusion constant, D , as a function on the noise intensity (and free diffusion constant), D_0 . The mean square displacement approaches asymptotically the Einstein law for any choice of D_0 . However, on increasing D_0 , the asymptotic diffusion constant, D , changes from

$$D = \kappa \sqrt{D_L D_0}, \quad (2.4)$$

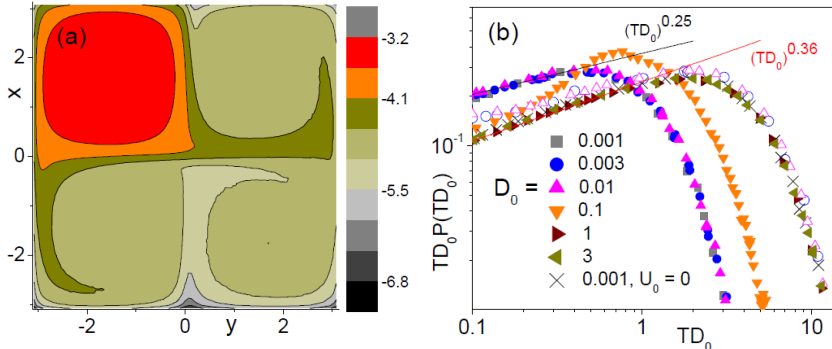


Figure 3: Exit mechanism from a flow cell: (a) Spatial distribution of a particle injected at the center of the top-left roll, $(-L/2, L/2)$, in a box with absorbing boundaries $x, y = \pm L/2$, and subjected to noise of strength $D_0 = 0.01$; the side-bar is the relevant amplitude color-code on a natural logarithmic scale. Distribution computed over 10^7 trajectories with integration time-step of 10^{-5} . (b) Distributions, $P(T)$, of the particle's exit times, T , for different D_0 (filled symbols, see legend). For a comparison (see text) the $P(T)$ curves for $D_0 = 3 \cdot 10^{-3}$ and 10^{-2} have been “stretched” by rescaling $T \rightarrow 4T$ (empty symbols). The stream function parameters are $U_0 = 1$ and $L = 2\pi$. Power laws are drawn to fit the $T \rightarrow 0$ branches of the low- and high-noise distributions. Note that in dimensionless units, simulation results for $U_0 = 0$ correspond to taking the limit $D_0 \rightarrow \infty$.

for $D_0 < D_L$ (dispersive transport), to

$$D = D_0 \quad (2.5)$$

for $D_0 > D_L$ (diffusive transport). The constant κ in Eq. (2.4) depends on the geometry of the flow cells (Rosenbluth 1987; Young et al. 1989). For the 2D array of square counter-rotating convection rolls of Eq. (2.1), $\kappa \simeq 1.06$ (Rosenbluth 1987), in close agreement with the numerical results displayed in Fig. 2.

The crossover between the two diffusion regimes occurs at $D_0 \simeq D_L$ and appears to be quite sharp (Li et al. 2020). This property was explained (Rosenbluth 1987; Soward 1987; Young et al. 1989) by noticing that for $D < D_L$ spatial diffusion occurs within the boundary flow layers delimiting the four subcells of the stream function, $\psi(x, y)$, as illustrated in Fig. 3(a). Stated otherwise, the diffusion process is governed by the advection velocity field. Vice versa, for $D_0 > D_L$ the effects of advection on the particle's diffusion grow negligible. In view of the above, NGND is more likely to happen in the regime of advective transport; therefore we focus our discussion on the high Péclet number domain.

3. Relevant Time Scales

The particle's dynamics of Eqs. (2.1)-(2.2) results from the superposition of an advective drag with velocity \vec{u} and a free Brownian motion driven by thermal fluctuations. Advection pulls the particle along closed orbits inside each $\psi(x, y)$ subcell, either clock- or anticlockwise, whereas thermal noise pushes the particle eventually over the subcell boundaries. Both mechanisms play a key role in our discussion of the ensuing NGND phenomenon. Therefore, in the next subsections we briefly derive their characteristic time scales.

3.1. Advection Period

To analyze roll circulation we consider the “positive” $\psi(x, y)$ subcell centered at $(L/4, L/4)$, see Fig. 1(a), where the particle circulates anticlockwise. In the noiseless regime with $D_0 = 0$, a

simple time derivation of both sides of Eqs. (2.1) yields two decoupled equations,

$$\ddot{x}' = \Omega_L^2 \sin x', \quad \ddot{y}' = \Omega_L^2 \sin y', \quad (3.1)$$

for the rescaled coordinates $x' = 2(2\pi x/L)$ and $y' = 2(2\pi y/L)$. Here the angular frequency $\Omega_L = 2\pi U_0/L$ coincides with the maximum vorticity, $\vec{\nabla} \wedge \vec{u} = -\nabla^2 \psi$, at the center of the convection roll. Both Eqs. (3.1) describe a mathematical pendulum centered at (π, π) – the subcell center. This implies that, due to the $x \leftrightarrow y$ symmetry of $\psi(x, y)$, the period of the particle's orbits, T_L , depends on their maximum amplitude, a_0 , along either x or y direction (orbits are not circular!) with $a_0 < \pi$. The function $T_L(a_0)$ can be expressed analytically as the period of either physical pendulum in Eq. (3.1),

$$T_L(a_0) = \frac{2T_0}{\pi} K(k), \quad (3.2)$$

where $T_0 = 2\pi/\Omega_L$, $k = \sin(a_0/2)$, and $K(k)$ is a complete elliptic integral of first kind (Cromer 1995). The logarithmic *divergence* of T_L for $a_0 \rightarrow \pi$ is best approximated by (Cromer 1995) $T_L = (2T_0/\pi) \ln[4/\cos(a_0/2)]$. This implies that, in the absence of thermal fluctuations, the particle gets trapped in a convection roll. Despite its simple derivation, our result for T_L is consistent with earlier estimates (Weiss 1966).

Under stationary conditions, the particle's spatial distribution is uniform, and so is the distribution of a_0 . Therefore, in the limit of very high Péclet numbers, $Pe \gg 1$, a useful estimate of the advection period can be obtained by averaging $T_L(a_0)$ with respect to a_0 , namely,

$$T_L = \langle T_L(a_0) \rangle = \frac{4T_0}{\pi} \int_0^1 \frac{K(k)}{k'} dk, \quad (3.3)$$

where $k' = \sqrt{1 - k^2}$. An explicit integration finally yields (Gradshteyn et al. 2007),

$$T_L = \frac{T_0}{4\pi^2} \Gamma^4(1/4) \simeq 4.4 T_0, \quad (3.4)$$

with Γ denoting a gamma function (Gradshteyn et al. 2007). In view of our derivation, it's clear that Eq. (3.4) only holds in the limit $D_0 \rightarrow 0+$. We reiterate that for $D_0 \equiv 0$ diffusion is completely suppressed.

3.2. Mean First-Exit Time

To estimate the Mean First-Exit Time (MFET) of the particle out of the flow unit cell, we calculate first the MFET of a free Brownian particle out of a square box of size L . In the absence of advection, $U_0 = 0$, this can be done analytically by standard stochastic methods – see Eq. (5.4.37) of Ref. (Gardiner 2009), where a typo had to be corrected. For a particle starting at (x_0, y_0) inside a box of vertices $x = \pm L/2$ and $y = \pm L/2$, the mean first-exit time is

$$T(x_0, y_0) = \frac{1}{D_0} \left(\frac{L}{2\pi} \right)^2 \left(\frac{8}{\pi} \right)^2 \sum_{m,n}^{(\text{odd})} \frac{1}{mn} \frac{1}{m^2 + n^2} \times \\ \times \sin \left[\pi n \left(\frac{x_0}{L} - \frac{1}{2} \right) \right] \sin \left[\pi m \left(\frac{y_0}{L} - \frac{1}{2} \right) \right], \quad (3.5)$$

where the summation is restricted to the odd values of m and n . Under stationary conditions, the spatial distribution of the particle is uniform. Therefore, we average $T(x_0, y_0)$ with respect to the particle's initial position, (x_0, y_0) , to obtain the spatially averaged MFET,

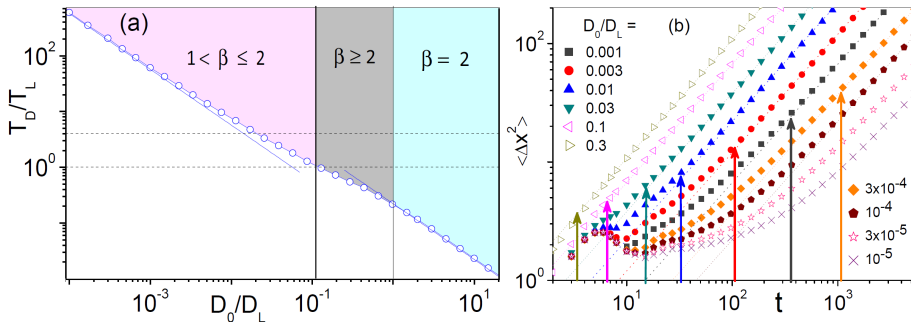


Figure 4: Diffusion mechanisms in the periodic flow pattern of stream function $\psi(x, y)$, Eq. (2.1): (a) T_D , vs. thermal noise, D_0 . The asymptotic solid lines on the left and right are respectively $\langle T(x_0, y_0) \rangle$ and $(1/4)\langle T(x_0, y_0) \rangle$, Eq. (3.6); the horizontal dashed lines represent the minimum, T_0 , (lower line) and the average advection period T_L of Eq. (3.4) (upper line). Three D_0 intervals with distinct ranges of the fitting parameter β of Eq. (4.1) are delimited by the vertical lines $D_0 = D^*$ and $D_0 = D_L$ and shaded in different colors; no NGND was detected for $D_0 > D_L$. D^* was obtained by numerically solving the equation $T_D = T_0$ (see txt). (b) $\langle \Delta x^2(t) \rangle$ vs. t for different D_0 . Vertical arrows denote the onset time of normal diffusion, $t = T_D$. Convection flow parameters are $U_0 = 1$ and $L = 2\pi$.

$$\langle T(x_0, y_0) \rangle = \frac{L^2}{D_0} \left(\frac{2}{\pi} \right)^6 \sum_{m,n}^{(\text{odd})} \frac{1}{m^2} \frac{1}{n^2} \frac{1}{m^2 + n^2}. \quad (3.6)$$

We next investigate the MFET for a Brownian tracer to escape from a unit cell of the stream function $\psi(x, y)$. Let T_D denote the spatial average of such a MFET, with spatial average taken over a unit flow cell. In the purely diffusive regime of Eq. (2.5), $D_0 \gg D_L$, the effect of advection is negligible; hence $T_D = \langle T(x_0, y_0) \rangle$. In the opposite limit of advective diffusion, $D_0 \ll D_L$, as apparent from Figs. 1(b) and 3(a), the exit process consists of a slow activation mechanism, where the particle thermally diffuses from the center of a subcell toward its boundaries, followed by a relatively faster propagation driven by the laminar flow, which runs parallel to the separatrices delimiting the adjacent counter-rotating subcells. This statement is based on the fact that, for $D_0 \rightarrow 0$, T_D diverges like $1/D_0$, Eq. (3.6), whereas T_L diverges like $T_L \sim (T_0/\pi) \ln(D_L/D_0)$. This last result follows from the logarithmic divergence of T_L in the limit $a_0 \rightarrow \pi$, which we derived in Sec. 3.1. There, $|\pi - a_0|$ was a measure of the particle's distance from the roll separatrices, which, in dimensional units, reads $\delta = (L/2\pi)|1 - a_0/\pi|$. In the presence of noise, the particle mean square displacement over the advection period T_0 gives a simple estimate of δ , $\delta^2 = 2D_0T_0$, which one may interpret as the effective width of the rolls' boundary flow layers (Rosenbluth 1987).

Consider now a particle trapped in a convection roll, say, in the top-left $\psi(x, y)$ subcell of Fig. 3(a). To leave the simulation box, it first slowly free diffuses inside the trapping subcell; it is only upon reaching the subcell boundary layer, that it gets swept away by the advection flow along the square net formed by the roll separatrices, as illustrated in Fig. 1(b). In the limit $D_0/D_L \rightarrow 0$, the advection period T_L grows negligible with respect to any exit diffusion time, so that the particle's MFET out of a unit $\psi(x, y)$ cell, T_D , tends to coincide with the particle's free diffusion time out of a single subcell. Such a latter time can be calculated by simply replacing L with $L/2$ in Eq. (3.6). In conclusion, we expect that for $Pe \gg 1$, $T_D = (1/4)\langle T(x_0, y_0) \rangle$. Our analytical estimates of T_D are in good agreement with the numerical data displayed in Fig. 4, which well illustrates the transition between the low- and high-noise regimes of T_D .

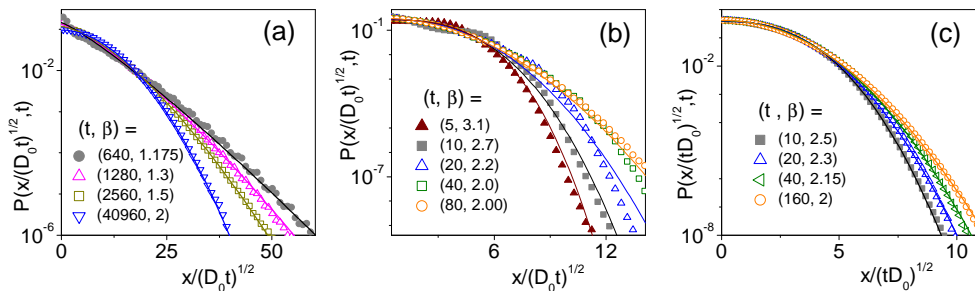


Figure 5: Rescaled displacement distributions for different transient times: (a) $D_0 = 0.001$, (b) $D_0 = 0.1$, and (c) $D_0 = 0.6$. The observation times, t , and the fitting parameters, β , are reported in the legends; convection flow parameters are $U_0 = 1$ and $L = 2\pi$. All transient pdf's were taken after normal diffusion was established, see Fig. 4(b).

Both limiting estimates for T_D ignore advection and, therefore, differ by just a geometric factor 4, that is the ratio of the cell-to-subcell areas. The predominance of this geometric factor is apparent also in Fig. 3(b), where first-exit time distributions, $P(T)$, have been plotted for low and high noise strengths. To numerically determine $P(T)$, first we computed the first-exit times, T , for a fixed starting point (x_0, y_0) ; then we averaged the relevant pdf's by taking a uniform distribution of (x_0, y_0) over a full unit flow cell. For the sake of a comparison, we also plotted the distributions for the two lowest values of D_0 on the dilated scale $T \rightarrow 4T$. The high-noise distributions, $P(T)$, and such “stretched” low-noise distributions, $P(4T)$, seemingly overlap, which corroborates our estimates of T_D in the limits $D_0 \rightarrow 0$ and $D_0 \rightarrow \infty$. Another interesting feature of the T distributions plotted in Fig. 3(b) is their behavior in the limit $T \rightarrow 0$. Our numerical data clearly show that for small T all distributions diverge according to a power law $T^{-\alpha}$, with α slowly decreasing with increasing D_0 , from $\alpha = 0.75$ to approximately $\alpha = 0.64$. The divergence of $P(T)$ for $T \rightarrow 0$ is dominated by the trajectories originating in the (sub)cell boundary layers; indeed, this effect disappears if we set the starting point (x_0, y_0) , say, at the center of the (sub)cells. At large T , all distributions decay exponentially, consistently with the asymptotic normal diffusion law of Eq. (2.3).

4. Results: Non-Gaussian Normal Diffusion

The Brownian particle diffuses in the x, y plane by jumping from convection roll to convection roll, thanks to thermal fluctuations. Therefore, its motion can be coarse grained as a discrete random walker with time constant T_D (Gardiner 2009). Accordingly, for large observation times, $t \gtrsim T_D$, the diffusive process is expected to be normal. This statement is confirmed by the numerical data for $\langle \Delta x^2(t) \rangle$ reported in Fig. 4(b), where the relevant T_D is indicated by vertical arrows. However, for $Pe \gg 1$ (very low thermal noise), we proved that $T_L < T_D$, that is the particle executes several orbits inside a single subcell before exiting it. Therefore, for short observation times, $t < T_D$, the particle is seen to travel distances of the order of the subcell half-width, $L/4$, and then turn back toward its starting point, with period of the order of T_0 . Such particle's intra-roll dynamics qualitatively explains magnitude and position of the short- t bumps clearly detectable in the $\langle \Delta x^2(t) \rangle$ curves of Fig. 4(b) at low D_0 . We notice that for $D_0 \rightarrow 0$ such bumps grow insensitive to D_0 , while the curve $\langle \Delta x^2(t) \rangle$ flattens out, as the particle gets trapped longer and longer inside a convection roll.

By contrast, for $t \gtrsim T_D$, $\langle \Delta x^2(t) \rangle$ follows a normal diffusion law with D in close agreement with the analytical prediction of Eq. (2.4). For the flow field parameters adopted in Fig. 5, the crossover between low- and high-noise estimates of T_D , respectively $(1/4)\langle T(x_0, y_0) \rangle$ and $\langle T(x_0, y_0) \rangle$, occurs

within the advective transport regime, $D_0 < D_L$. By inspecting Fig. 4(a), it is also apparent that at the crossover the two competing time scales introduced in Sec. 3 to characterize the particle dynamics in a convective roll, tend to coincide. The equation $T_D = T_0$ defines a unique D_0 value, D_* , which splits the advective diffusion domain into the two distinct intervals $D_0 < D_*$ and $D_* < D_0 < D_L$.

Similarly to other low-dimensional models (Li et al. 2020), numerical integration of Eqs. (2.1)-(2.2) shows compelling evidence of the NGND phenomenon, with the non-Gaussian transients of the displacement distributions gradually disappearing upon increasing the observation time. Contrary to superstatistical (Wang et al. 2009) and diffusing diffusivity models (Chubynsky et al. 2014), here the predicted transient rescaled distributions are not “universal” D functions over large t intervals. Accordingly, to capture the t dependence of the numerical curves presented in Fig. 5, one needs at least one additional fitting parameter. To this purpose, we introduced and tested the following one-parameter fitting function,

$$p_\beta \left(\frac{\Delta x}{\sqrt{t}} \right) = \frac{\beta}{\Gamma(\frac{1}{\beta})^{\frac{3}{2}}} \left[\frac{\Gamma(\frac{3}{\beta})}{2D} \right]^{\frac{1}{2}} \exp \left[- \left(\frac{\Delta x^2}{2Dt} \frac{\Gamma(\frac{3}{\beta})}{\Gamma(\frac{1}{\beta})} \right)^{\frac{\beta}{2}} \right]. \quad (4.1)$$

This function has been derived phenomenologically starting from the stretched exponential distribution, $p_\beta(\Delta x/\sqrt{t}) = A \exp[-B(\Delta x/\sqrt{t})^\beta]$ (Kendall et al. 1976). The constants A and B have then be determined by normalizing $p_\beta(\Delta x/\sqrt{t})$ to one and ensuring that its second moment be $\langle \Delta x^2 \rangle/t = 2D$ for any value of the free parameter β , which, instead, is allowed to vary with t . β assumes values in the range $1 \leq \beta \leq 2$ for leptokurtic distributions (positive excess kurtosis) and $\beta \geq 2$ for platykurtic distributions (negative excess kurtosis).

The fits of the pdf’s drawn in Fig. 5 have been generated from Eq. (4.1) by setting D equal to the diffusion constant that best fitted the corresponding diffusion data of Fig. 4(b) at large t and, then, computing β to best fit the rescaled displacement distributions numerically obtained for different t . For an easier comparison with the experimental data we used there the rescaled observable $\Delta x/\sqrt{tD_0}$.

The range of the β values, fitted according to this procedure, is reported in Fig. 4(a) for each D_0 interval. As corroborated by the transient pdf’s displayed in Fig. 5, NGND transients are leptokurtic for $D_0 < D_*$ and platykurtic for $D_* < D_0 < D_L$ (Kendall et al. 1976). This interesting property can be explained with the fact that in the present system the role of transient time, τ , is played respectively by T_D for $D_0 < D_*$ and by T_L for $D_0 > D_*$. In particular, for $D_0 > D_*$ the slowest time modulation of the particle’s dynamics is attributable to the advective circulation inside the convection rolls, $T_L > T_D$, which explains the emergence of a platykurtic NGND transient. Indeed, a microscopic rotational (random) dynamics suffices to determine sub-Gaussian distributions, i.e., a negative excess kurtosis, of the unidirectional particle’s displacements (Zheng et al. 2013).

As far as the quality of the proposed fitting procedure is concerned, we notice that it is quite accurate in both limits, $D_0 \ll D_*$ and $D_0 \gg D_*$, where the effective transient time, τ , can be positively identified respectively with T_D and T_L . For intermediate values of D_0 , $D_0 \sim D_*$, the one-parameter function $p_\beta(\Delta x/\sqrt{t})$ seems to provide less accurate fits of the numerical data, see Fig. 5(b).

5. Conclusions

The diffusive model investigated in this paper provides a suggestive example of low dimensional system exhibiting NGND. As an additional peculiarity, its transient displacement distributions can be either leptokurtic or platykurtic, depending on the choice of the model’s parameters. Variations

of this system are plenty. For instance, one could design different convective roll patterns or consider roll arrays in confined geometries (Shraiman 1987; Young et al. 1989). Also interesting would be replacing the passive Brownian particle in Eqs. (2.1) with a self-propelling swimmer (Li et al. 2020). All these systems are likely to manifest the NGND phenomenon. In view of the growing attention to the diffusion of active particles, we will report on NGND of microswimmers in convection rolls in a forthcoming publication. Finally, we remark that all these diffusive systems are easily accessible to direct experimental observation (Solomon 2003; Young 2007; Li et al. 2020).

Acknowledgements

Y.L. is supported by the NSF China under grants No. 11875201 and No. 11935010. P.K.G. is supported by SERB Start-up Research Grant (Young Scientist) No. YSS/2014/000853 and the UGC-BSR Start-Up Grant No. F.30-92/2015.

Conflict of interest:

The authors declare that they have no conflict of interest.

Availability of data

The data that support the findings of this study are available from the corresponding author upon reasonable request.

REFERENCES

- BHATTACHARYA, S., SHARMA, D. K., SAURABH, S., DE, S., SAIN, A., NANDI, A., AND CHOWDHURY, A. 2013 Plasticization of poly(vinylpyrrolidone) thin films under ambient humidity: Insight from single-molecule tracer diffusion dynamics, *J. Phys. Chem. B* **117**, 7771.
- CHANDRASEKHAR, S. 1967 *Hydrodynamic and Hydromagnetic Stability* (Oxford University Press, New York).
- CHAUDHURI, P., BERTHIER, P. AND KOB, W. 2007 Universal nature of particle displacements close to glass and jamming transitions. *Phys. Rev. Lett.* **99**, 060604.
- CHILDRESS, S. 1979 Alpha-effect in flux ropes and sheets. *Phys. Earth Planet. Int.* **20**, 172.
- CHUBYNSKY M. V. AND SLATER, G. W. 2014 Diffusing diffusivity: A model for anomalous, yet Brownian, diffusion, *Phys. Rev. Lett.* **113**, 098302 .
- CROMER N. O. 1995 Many oscillations of a rigid rod. *Am. J. Phys* **63**, 112 (1995).
- EAVES, J. D. AND REICHMAN, D. R. 2009 Spatial dimension and the dynamics of supercooled liquids. *Proc. Natl. Acad. Sci. U.S.A.* **106**, 15171.
- GARDINER, C. *Stochastic Methods: A Handbook for the Natural and Social Sciences* (Springer, Berlin, 2009).
- GHOSH, S. K., CHERSTVY, A. G., GREBENKOV D. S., AND METZLER, R. 2016 Anomalous, non-Gaussian tracer diffusion in crowded two-dimensional environments, *New J. Phys.* **18**, 013027.
- GRADSHTEYN I. S. AND RYZHIK, I. M. 2007 *Table of Integrals, Series, and Products*, 7th Edition (Academic Press, 2007).
- GUAN, J., WANG, B. AND GRANICK, S. (2014) Even hard-sphere colloidal suspensions display Fickian yet non-Gaussian diffusion, *ACS Nano* **8**, 3331.
- HE, W., SONG, H., SU, Y., GENG, L., ACKERSON, B. J., PENG, H. B., AND TONG, P. Dynamic heterogeneity and non-Gaussian statistics for acetylcholine receptors on live cell membrane. *Nat. Comm.* **7**, 11701.
- KEGEL W. K. AND VAN BLAADEREN, A. 2000 Direct observation of dynamical heterogeneities in colloidal hard-sphere suspensions. *Science* **287**, 290 .
- KENDALL M. G. AND STUART, A. 1976 *The Advanced Theory of Statistics*, Volume 1, 3rd Edition, (London, Griffin&Co, 1976).
- KIM, J., KIM, C., AND SUNG, B. J. 2013 SIMULATION STUDY OF SEEMINGLY FICKIAN BUT HETEROGENEOUS DYNAMICS OF TWO DIMENSIONAL COLLOIDS, *Phys. Rev. Lett.* **110**, 047801.

- KIRBY, B. J. 2010 *Micro- and Nanoscale Fluid Mechanics: Transport in Microfluidic Devices* (Cambridge University Press).
- KLOEDEN, P. E. AND PLATEN, E. 1992 *Numerical Solution of Stochastic Differential Equations* (Springer).
- KWON, G., SUNG, B. J. AND YETHIRAJ A. 2014 Dynamics in crowded environments: Is non-Gaussian Brownian diffusion normal? *J. Phys. Chem. B* **118**, 8128.
- LEPTOS, K. C., GUASTO, J. S., GOLLUB, J. P., PESCI, A. I. AND GOLDSTEIN, R. E. 2009 Dynamics of enhanced tracer diffusion in suspensions of swimming eukaryotic microorganisms. *Phys. Rev. Lett.* **103**, 198103 (2009).
- LI, Y., MARCHESONI, F., DEBNATH, D. AND GHOSH, P. K. 2019 Non-Gaussian normal diffusion in a fluctuating corrugated channel, *Phys. Rev. Res.* **1**, 033003.
- LI, Y. LI, L., MARCHESONI, F., DEBNATH, D., AND GHOSH, P. K. 2020 Active diffusion in convection rolls, *Phys. Rev. Res.* **2**, 013250 (2020).
- MANIKANTAN, H. AND SAINTILLAN, D. 2013 Subdiffusive transport of fluctuating elastic filaments in cellular flows, *Phys. Fluids* **25**, 073603.
- MOFFATT, H. K., ZASLAVSKY, G. M., COMTE, P. AND TABOR TABOR M. (Eds.) 1992 *Topological Aspects of the Dynamics of Fluids and Plasmas* (Springer Netherlands).
- ROSENBLUTH, M. N., BERK, H. L., DOXAS, I. AND HORTON, W. 1987 Effective diffusion in laminar convective flows. *Phys. Fluids* **30**, 2636 (1987).
- SARRACINO, A., CECCONI, F., PUGLISI, A. AND VULPIANI, A. 2016 Nonlinear response of inertial tracers in steady laminar flows: Differential and absolute negative mobility, *Phys. Rev. Lett.* **117**, 174501 (2016).
- SHRAIMAN, B. I. 1987 Diffusive transport in a Rayleigh-Bénard convection cell, *Phys. Rev. A* **36**, 261.
- SOLOMON T. H. AND GOLLUB, J. P. 1988 Chaotic particle transport in time-dependent Rayleigh-Bénard convection, *Phys. Rev. A* **38**, 6280.
- SOLOMON T. H. AND MEZIĆ, I. 2003 Uniform resonant chaotic mixing in fluid flows, *Nature (London)* **425**, 376 (2003).
- SOWARD, A. M. 1987 Fast dynamo action in a steady flow. *J. Fluid Mech.* **180** 267.
- TABELING, P. 2002 Two-dimensional turbulence: a physicist approach. *Phys. Rep.* **362**, 1.
- TORNEY C. AND NEUFELD, Z. 2007 Transport and aggregation of self-propelled particles in fluid flows, *Phys. Rev. Lett.* **99**, 078101 (2007)
- WANG, B., ANTHONY, S. M., BAE, S. C. AND GRANICK, S. 2009 Anomalous yet Brownian *Proc. Natl. Acad. Sci. U.S.A.* **106**, 15160.
- WANG, B., KUO, J., BAE, C., AND GRANICK S. 2012 When Brownian diffusion is not Gaussian, *Nat. Mater.* **11**, 481.
- WEISS, N. O. 1966 The expulsion of magnetic flux by eddies, *Proc. Roy. Soc.* **A293**, 310 (1966).
- WEEKS, E. R., CROCKER, J. C., LEVITT, A. C., SCHOFIELD, A., WEITZ, D. A. 2000 Three-dimensional direct imaging of structural relaxation near the colloidal glass transition, *Science* **287**, 627.
- YOUNG, W., PUMIR, A., AND POMEAU, Y. 1989 Anomalous diffusion of tracer in convection rolls, *Phys. Fluids A* **1**, 462).
- YOUNG, Y.-N. AND SHELLEY, M. J. 2007 Stretch-coil transition and transport of fibers in cellular flows, *Phys. Rev. Lett.* **99**, 058303.
- ZHENG, TEN HAGEN, B., KAISER, A., WU, M., CUI, H., SILBER-LI, Z. AND LÖWEN, H. 2013 Non-Gaussian statistics for the motion of self-propelled Janus particles: experiment versus theory, *Phys. Rev. E* **88**, 032304.